THE ASTROPHYSICAL JOURNAL, 470:806–813, 1996 October 20

ON THE HOST GALAXIES OF THE GIGAHERTZ PEAKED-SPECTRUM RADIO SOURCES

CHRISTOPHER P. O'DEA
Space Telescope Science Institute,[1] 3700 San Martin Drive, Baltimore, MD 21218; odea@stsci.edu
CARLO STANGHELLINI
Istituto di Radioastronomia del CNR, Noto, Italy; carlo@eloro.ira.noto.cnr.it
STEFI A. BAUM
Space Telescope Science Institute,[1] 3700 San Martin Drive, Baltimore, MD 21218; sbaum@stsci.edu
AND
STEPHANE CHARLOT
Institut d'Astrophysique, Paris, France; charlot@iap.fr
Received 1996 January 16; accepted 1996 May 10

ABSTRACT

We discuss the results of broadband optical imaging of the host galaxies of a sample of 40 GHz peaked-spectrum (GPS) radio galaxies. The GPS galaxies have absolute magnitudes in the R_C band between -22 and -24.0, consistent with brightest cluster galaxies and the hosts of other powerful radio sources. The GPS Hubble diagram and the redshift distribution of $r - i$ colors are consistent with both no-evolution models and passive evolution models for elliptical galaxies. The GPS galaxies are in good agreement with the R_C band Hubble diagram for 3CR galaxies at low redshifts, $z \lesssim 0.5$. At higher redshifts, there is a suggestion that the GPS galaxies are about 1 mag fainter than the 3CR galaxies. If real, this may be due to 3CR galaxies having an extra component of blue light (the aligned component?) that is not present in the GPS galaxies. We suggest that the presence or lack of the blue light may be related to the presence or lack of a powerful *extended* radio source.

Subject headings: galaxies: evolution — radio continuum: galaxies

1. INTRODUCTION

GHz peaked-spectrum (GPS) radio galaxies (O'Dea, Baum, & Stanghellini 1991) make up significant fractions ($\sim 10\%$) of the bright centimeter-wavelength–selected radio source population but are not well understood. They are powerful but compact radio sources, the spectra of which are simple and convex, with a peak near 1 GHz. The GPS sources are entirely contained within the extent of the narrow-line region ($\lesssim 1$ kpc).

There are several hypotheses for the origin of GPS sources.

1. They could be radio galaxies in the early stages of their lives (Phillips & Mutel 1982; Carvalho 1985; Hodges & Mutel 1987; De Young 1993; Fanti et al. 1995; Readhead et al. 1996a, 1996b). In this scenario, they might ultimately become large-scale powerful Fanaroff & Riley (1974) class 2 (FR2) radio sources or perhaps weaker (FR1) sources if they decline in luminosity as they age.
2. They could be confined to their present size scale via interaction with their ambient medium (see, e.g., van Breugel, Miley, & Heckman 1984; Wilkinson et al. 1984; Fanti et al. 1990; Baum et al. 1990; O'Dea et al. 1991; Carvalho 1994). These "frustrated" sources never become large-scale doubles.
3. They might be short-lived phenomena that occur in most $L \gtrsim 0.3L_*$ galaxies (Readhead et al. 1994).

The presence of the GPS radio galaxies at redshifts $0.1 \lesssim z \lesssim 1$, and their absence at lower redshifts (O'Dea et al. 1991),[2] suggests that their origin and evolution may be tied to the dynamical evolution of galaxies and their cluster environments at these epochs. The optical properties of the host galaxies of GPS sources can provide clues to the nature and origin of these sources. In this paper, we discuss the absolute magnitudes and colors of the GPS galaxies and their behavior on the Hubble diagram.

2. THE SAMPLE

The sample of GPS sources is described by O'Dea et al. (1991), O'Dea et al. (1996), and De Vries et al. (1996). The sources are selected on the basis of their peaked spectrum between about 0.5 and 5.0 GHz. The sources are drawn from several flux density–limited high-frequency–selected samples (Peacock & Wall 1982 at 2.7 GHz; Pauliny-Toth et al. 1978 and Kuhr et al. 1981a, 1981b at 5 GHz). The optical imaging is somewhat inhomogenous, coming from several different groups (see, e.g., Stanghellini et al. 1993; O'Dea, Baum, & Morris 1990a; Biretta, Schneider, & Gunn 1985; De Vries, Barthel, & Hes 1995; Fugmann, Meisenheimer, & Röser 1988; Stickel & Kuhr 1994; Snellen et al. 1996).

In order to study the host galaxy properties, we have selected all the GPS radio *galaxies* for which there is at least one CCD image in at least one band. The final sample consisted of 40 GPS galaxies. Deep CCD images are necessary to derive the host galaxy properties since the host galaxies are at intermediate redshifts and are thus fairly faint. Because of the large amount of recent CCD observations of

[1] Operated by the Association of Universities for Research in Astronomy, Inc., under contract with the National Aeronautics and Space Administration.

[2] Note that unlike the GPS galaxies that are found at moderate redshifts, $0.1 \lesssim z \lesssim 1$, the GPS quasars tend to be found at high redshift, $2 \lesssim z \lesssim 4$ (O'Dea 1990; Peterson et al. 1982).

GPS galaxies, it turns out that the requirement that the object in this sample have a CCD image is not really restrictive. Only one of the objects classified as a galaxy in the O'Dea et al. (1991) sample is left out in the current work because of lack of an available CCD image (2323+790). The new data have allowed us to revise some of the earlier object classifications. The objects discussed in this paper are all classified as galaxies, and this classification supersedes that in O'Dea et al. (1991). Table 1 gives the observed optical properties of the sample. Note that in some cases the redshifts are not known for the GPS galaxies; thus, it is not possible to determine the magnitude within a standard linear aperture or within some absolute isophotal level. Thus, the magnitudes correspond to the "total extent" of the galaxy visible on the CCD image.

2.1. *Determining Magnitudes in a Consistent Manner*

The distribution of absolute magnitudes is of fundamental importance since it will tell us how the host galaxies of the GPS sources are related to those of the large-scale

TABLE 1

OBSERVED PROPERTIES OF GPS RADIO GALAXIES

Source[a] (1)	z[b] (2)	Red Magnitude[c] (3)	System[d] (4)	$r-i$[e] (5)	Morphology[f] (6)	Separation (arcsec)[g] (7)	Separation (kpc)[h] (8)	References (9)
0018+729.....	0.821?	22.4	G	1.5	a	1.1	8	1, 2
0019−000.....	0.305	18.4	G	0.4	b, c	8.3	33	1, 2
0022−423.....	0.937	20.3	Gi	...	c	17	118	3
0026+346.....	...	20.2	G	...	f	...	...	4, 5
0108+388.....	0.669	22.0	G	1.2	a	15.6	94	1, 6
0316+161.....	...	23.6	C	...	c, f	1.7	...	1, 7
0404+768.....	0.599	21.1	G	1.7	c	6.1	35	1, 6
0428+205.....	0.219	19.3	C	...	a, c	4.3	13	1, 8
0500+019.....	0.583	21.2	C	...	a, c, d	1.7	10	3, 7, 9
0554−026.....	...	19.1	G	...	c	8.3	...	1, 3
0602+780.....	...	22.0	G	0.7	c, f	10.2	...	1
0710+439.....	0.518	19.84	G	0.76	a, d	3.7	20	1, 6, 10, 11
0914+114.....	...	20.0	G	0.5	...	18.0	...	1
0941−080.....	...	17.9	G	1.0	b	2.5	...	1
1031+567.....	0.459	20.2	G	...	a, d	13.0	65	1, 12, 13
1117+146.....	0.362	20.1	C	...	a, c, d	7.2	32	3
1323+321.....	0.369	19.2	G	0.4	a, d	9.0	39	1, 12
1345+125.....	0.122	15.5	G	0.3	a, b, d	2.2	4.4	1, 10, 14
1358+624.....	0.431	19.8	G	0.3	a, c	3.0	14	1
1404+286.....	0.077	14.6	G	0.2	a, c	10.2	13	1, 15
1433−040.....	...	22.3	G	0.2	f	...	...	1
1543+005.....	...	20.0	M	...	c	6.0	...	16
1600+335.....	...	23.2	G	0.5	a, c	3.8	...	1, 5
1604+315.....	...	22.7	G	1.4	a, d	1.1	...	1
1607+268.....	0.473	20.4	G	0.6	a, d	6.0	32	1, 17, 18
1732+094.....	...	20.7	M	...	a, c	4.0	...	16
1751+278.....	...	21.7	M	...	c	7.4	...	16
1843+356.....	0.765	21.9	G	...	c	5.6	...	1, 2
1934−638.....	0.183	17.2	C	...	b	2.8	8	2, 19
2008−068.....	...	21.3	M	...	a, c	2.0	...	1, 7, 16
2021+614.....	0.2266	18.1	G	0.6	c, e	6.7	21	16, 17, 20
2050+364.....	0.354	21.2	G	0.1	c	2.2	9	16, 17, 21
2121−014.....	1.158	22.7	Gi	...	f	...	...	2, 16
2128+048.....	0.990	23.3	G	1.5	c, f	4.0	...	5, 17
2149+056.....	0.740	20.4	M	...	a, c, e	11.0	68	16, 22, 23
2210+016.....	...	21.0	Gi	...	f	...	...	3, 7
2322−040.....	...	23.5	G	0.6	a	1.0	...	1, 24
2333−528.....	...	21.8	Gi	...	f	...	...	3
2337+264.....	...	20.0	Gi	...	f	...	...	3
2352+495.....	0.237	18.4	M	...	c, d	8.2	28	6, 16

[a] IAU name in B1950 coordinates.

[b] Heliocentric optical redshift.

[c] "Red" magnitude uncorrected for Galactic extinction.

[d] The magnitude system of the red magnitude. G is Gunn r, Gi is Gunn i, M is Mould R, C is Cousins R_C.

[e] $r-i$ color in Gunn system uncorrected for Galactic extinction.

[f] Comments on morphology and environment following Stanghellini et al. 1993: (a) distorted, (b) probable double nucleus, (c) possible companions, (d) possible member of group or cluster, (e) N galaxy (bright nucleus), (f) not enough signal-to-noise ratio to tell if the galaxy is distorted.

[g] Projected separation in arcsec to nearest possible companion or second nucleus.

[h] Projected separation in kpc to nearest possible companion or second nucleus.

REFERENCES.—(1) Stanghellini et al. 1993; (2) Snellen et al. 1996; (3) de Vries, Barthel, & Hes 1995; (4) Peacock et al. 1981; (5) Stickel et al. 1996; (6) Lawrence et al. 1986, 1987, 1996; (7) Fugmann, Meisenheimer, & Röser 1988; (8) Hewitt & Burbidge 1991; (9) Stickel et al. 1996; (10) Hutchings 1987, Hutchings, Johnson, & Pyke 1988; (11) G. Taylor 1995, private communication; (12) Dunlop et al. 1989; (13) Meisenheimer & Röser 1983; (14) Gilmore & Shaw 1986, Shaw, Tzioumis, & Pedlar 1992; (15) Jiménez 1987 and references therein; (16) O'Dea, Baum, & Morris 1990a; (17) Biretta et al. 1985; (18) Porcas 1990; (19) Jauncey et al. 1986, Fosbury et al. 1987; (20) Bartel et al. 1984; (21) O'Dea et al. 1996; (22) Stickel & Kühr 1993; (23) Fugmann & Meisenheimer 1988; (24) O'Dea et al. 1992.

powerful radio galaxies. Here we discuss the estimation of the absolute magnitudes in the Cousins R_C band.

We have compiled "red" magnitudes for all the galaxies in Table 1. These are usually Gunn r but also include Gunn i, Cousins R_C, and Mould R. We have preferentially used data from our own work (Stanghellini et al. 1993) where possible. We have applied the following corrections to the data in order to transform them to a uniform set of absolute magnitudes in the Cousin R_C band (see Table 2). The uncertainties in the various corrections probably add an additional uncertainly of a few tenths of a magnitude to the final absolute magnitude.

2.1.1. *Reddening Corrections*

We corrected the magnitudes using the values of $E(B-V)$ derived from the contour plots of Burstein & Heiles (1982). We converted the $E(B-V)$ to an extinction using the average extinction curve of Savage & Mathis (1979) [which gives a standard V-band extinction of $A(V) = 3.1E(B-V)$] by interpolating to the central wavelengths of our r and i filters. We derive extinctions of $A(\text{Gunn } r) = 2.5E(B-V)$, $A(\text{Gunn } i) = 1.8E(B-V)$.

2.1.2. *Transformations to Cousin R_C*

We used the colors for an elliptical galaxy in various filter systems given in Table 3 of Frei & Gunn (1994) to transform the available red magnitudes to R_C. This assumes that the colors of these GPS galaxies are similar to those of simple elliptical galaxies (which is consistent with our results below in § 3.4, with only a couple of notable

TABLE 2

CORRECTED COLORS, MAGNITUDES, AND ABSOLUTE MAGNITUDES

Source[a] (1)	l[b] (2)	b[c] (3)	$E(B-V)$[d] (4)	Red Magnitude[e] (5)	$r-i$[f] (6)	R_C[g] (7)	$M(R_C)$[h] (8)
0018+729.....	120.74	10.47	0.36	21.5	1.2	21.2	−23.7
0019−000.....	107.46	−61.75	0.01	18.4	0.4	18.1	−23.0
0022−423.....	321.35	−74.12	0.00	20.3	...	20.8	−24.9
0026+346.....	117.79	−27.71	0.06	20.1	...	19.8	...
0108+388.....	127.20	−23.60	0.06	21.9	1.2	21.6	−22.3
0316+161.....	166.64	−33.60	0.09	23.4	...	23.4	...
0404+768.....	133.41	18.33	0.15	20.7	1.6	20.4	−23.0
0428+205.....	176.81	−18.56	0.42	18.2	...	18.2	−22.0
0500+019.....	197.91	−22.81	0.09	21.0	...	21.0	−22.3
0554−026.....	209.06	−13.36	0.45	18.0	...	17.7	...
0602+780.....	135.89	24.41	0.09	21.8	0.6	21.5	...
0710+439.....	173.79	22.20	0.09	19.6	0.5	19.3	−23.5
0914+114.....	219.62	37.41	0.01	20.0	0.5	19.7	...
0941−080.....	244.07	32.35	0.03	17.8	1.0	17.5	...
1031+567.....	153.05	51.93	0.01	20.2	...	19.9	−22.5
1117+146.....	239.45	65.26	0.03	20.0	...	20.0	−21.6
1323+321.....	67.23	81.05	0.00	19.2	0.4	18.9	−22.7
1345+125.....	347.22	70.17	0.00	15.5	0.3	15.2	−23.5
1358+624.....	109.59	53.13	0.01	19.8	0.3	19.5	−22.7
1404+286.....	41.86	73.25	0.00	14.6	0.2	14.3	−23.3
1433−040.....	345.67	49.79	0.03	22.2	0.2	21.9	...
1543+005.....	7.87	40.33	0.09	19.8	...	20.1	...
1600+335.....	53.73	48.71	0.01	23.2	0.5	22.9	...
1604+315.....	50.82	47.66	0.01	22.7	1.4	22.4	...
1607+268.....	44.17	46.20	0.03	20.3	0.6	20.0	−22.5
1732+094.....	32.86	21.25	0.12	20.4	...	20.7	...
1751+278.....	53.09	24.29	0.06	21.5	...	21.8	...
1843+356.....	65.05	16.53	0.09	21.7	...	21.4	−23.2
1934−638.....	332.75	−29.39	0.06	17.0	...	17.0	−22.7
2008−068.....	36.01	−20.80	0.09	21.1	...	21.4	...
2021+614.....	96.08	13.78	0.24	17.5	0.4	17.2	−23.1
2050+364.....	78.86	−5.12	...	...	...	...	...
2121−014.....	51.35	−33.92	0.06	22.6	...	23.1	−23.8
2128+048.....	58.65	−31.81	0.06	23.2	1.5	22.9	−23.1
2149+056.....	63.31	−35.44	0.03	20.3	...	20.6	−23.8
2210+016.....	63.68	−42.02	0.03	20.9	...	21.4	...
2322−040.....	77.78	−58.84	0.01	23.5	0.6	23.2	...
2333−528.....	326.68	−60.91	0.00	21.8	...	22.3	...
2337+264.....	103.87	−33.53	0.06	19.9	...	20.2	...
2352+495.....	113.71	−12.03	0.24	17.8	...	18.1	−22.3

[a] Name.
[b] Galactic longitude.
[c] Galactic latitude.
[d] $E(B-V)$ determined from the contour plots of Burstein & Heiles 1982.
[e] Red magnitude from Table 1 (col. [4]) corrected for Galactic extinction. The average extinction curve of Savage & Mathis 1979 was used and interpolated to the center wavelengths of the different filters giving the extinctions $A(\text{Gunn } r) = 2.5E(B-V)$, $A(\text{Mould } R \text{ and Cousins } R_C) = 2.6E(B-V)$, and $A(\text{Gunn } i) = 1.8E(B-V)$.
[f] Gunn $r-i$ color corrected for Galactic extinction as described in the notes for col. [4].
[g] The apparent Cousin R_C magnitude determined using conversions from Frei & Gunn 1994 as described in the text.
[h] Absolute Cousins R_C magnitude for those sources with a measured redshift.

exceptions).

Based on the data of Frei & Gunn, the transformation is

$$R_C \simeq r - 0.305 + 0.025(r - i) . \quad (1)$$

For galaxies with only a single magnitude (either r or i) and a redshift, we adopted the $r - i$ color appropriate to that redshift. The color term is small, so uncertainties in the $r - i$ color will have a negligible effect on the Cousins R magnitude. If the redshift is unknown, we adopted the "typical" $r - i$ color $r - i = 0.45$, which is acceptable since over the redshift range 0.0–0.6, the $R_C - r$ color is not a strong function of redshift or of $r - i$ color (Frei & Gunn 1994). However, the sources with unknown redshift are ignored in the discussions in § 3 on the absolute magnitude, Hubble diagram, and $r - i$ color versus redshift, so the assumption of an $r - i$ color for these sources has absolutely no effect on our conclusions below.

2.1.3. *K-Correction*

Frei & Gunn (1994) do not provide K-corrections beyond a redshift of 0.6. We used the redshift-dependent (no correction for stellar evolution) K-correction for the Coleman, Wu, & Weedman (1980) E/S0 spectral energy distribution calculated by H. C. Ferguson (1995, private communication) that covers the entire redshift range of the GPS galaxies. This calculation uses the Johnson R bandpass as given by Bruzual (1981) and the zero point from R. L. Kurucz (unpublished). Ferguson's K-correction in the Johnson R is in good agreement with that from Frei & Gunn (1994) for the Cousins R_C over the redshift range $z \lesssim 0.6$. The difference is negligible at low redshifts and increases to 0.1 mag at $z = 0.6$. Note that the no-evolution model is a good description of the R_C band Hubble diagram and the redshift dependence of the $r - i$ colors (see below). Thus, the adopted K-correction is certainly adequate for our purposes.

3. DISCUSSION

3.1. *Are GPS Galaxies Interacting?*

In Table 1, we characterize the morphology of the sample of galaxies. There are 30 objects for which there is sufficient signal-to-noise ratio that we can determine the basic morphology. The observations used generally reach a sensitivity (i.e., lowest [3 σ] contour level) of about 24.5 mag arcsec^{-2} (observed) in the r band. We find that 17 of these objects (57%) have distorted isophotes and that four galaxies (13%) have a second nucleus in projection (within a few arcsec or within 10 kpc).

Other studies of powerful radio galaxies have found similar fractions of distorted objects (see, e.g., Heckman et al. 1986; Smith & Heckman 1989a, 1989b). Smith & Heckman (1989b) found similarly high fractions (54%) with distorted isophotes and (20%) with double nuclei in their sample of powerful radio galaxies at surface brightness levels (in the rest frame) brighter than 25 mag arcsec^{-2}. Thus, our results for the morphologies of GPS radio galaxies are consistent with those found for the powerful radio galaxies with extended radio structure. We find that a large fraction of the GPS radio galaxies show evidence for interaction and/or mergers and surmise that these processes must be relevant to or at least associated with the formation of GPS radio sources. We note that at low redshift, FR2 galaxies tend to exhibit signs of interaction much more often than FR1 galaxies (Heckman et al. 1986; Smith & Heckman 1989b; Baum & Heckman 1989; Ledlow & Owen 1995). Thus, the GPS hosts are more like FR2 hosts than FR1 in this property.

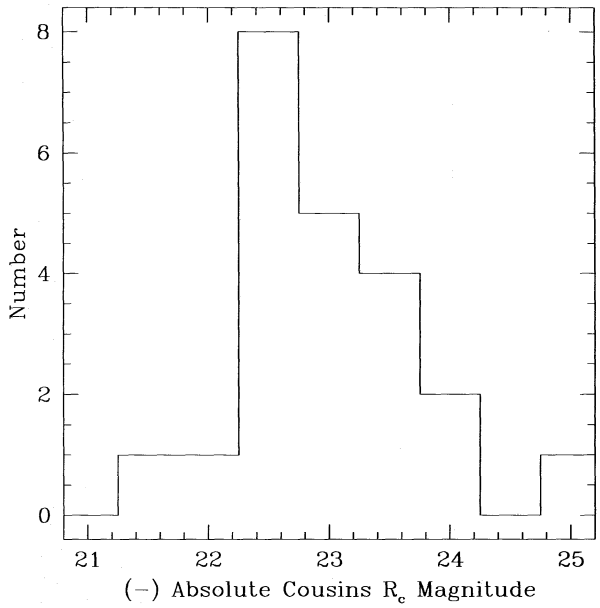

FIG. 1.—Distribution of absolute Cousins R_C magnitudes for GPS host galaxies.

We have determined the projected distance to the closest *apparent* companion or second nucleus of the GPS galaxies.[3] We do not have redshifts yet for these possible companions, so their relationship to the GPS source is currently unknown. The derived angular and linear separations are given in Table 1. The median angular separation is $\sim 5''$, and the median linear separation is ~ 20 kpc. If these possible companions are confirmed, then their relative closeness to the GPS galaxy is consistent with the other evidence that these sources are interacting and/or merging.

3.2. *Absolute Magnitudes*

The absolute magnitudes (for those sources with known redshifts) in R_C are given in Table 2 and Figure 1. The bulk of the magnitudes are between -22 and -24.0 (which corresponds to the range from M_* to 2 mag brighter). This range of absolute magnitudes is consistent with the host galaxies of other powerful radio galaxies (see, e.g., Owen & Laing 1989; Owen & White 1991; Smith & Heckman 1989b) and first-ranked cluster galaxies (Postman & Lauer 1995). Thus, the distribution of optical absolute magnitudes is at least consistent with these sources being the progenitors of the large-scale radio sources. Note, however, that examination of the R_C Hubble diagram below does reveal differences between the GPS and 3CR host galaxies.

3.3. *The* R_C-Band Hubble Diagram

Figure 2 shows the R_C-band Hubble diagram for both the GPS sources and powerful *extended* radio galaxies (mostly from 3CR). The GPS Hubble diagram has also been discussed by Stanghellini (1992), de Vries (1995), and Snellen et al. (1996). The good agreement between the GPS and extended radio galaxies (especially at $z \lesssim 0.5$) suggests that to first order the host galaxies of the GPS sources and

[3] We adopt a Hubble constant of $H_0 = 75$ km s^{-1} Mpc^{-1} and $q_0 = 0.0$.

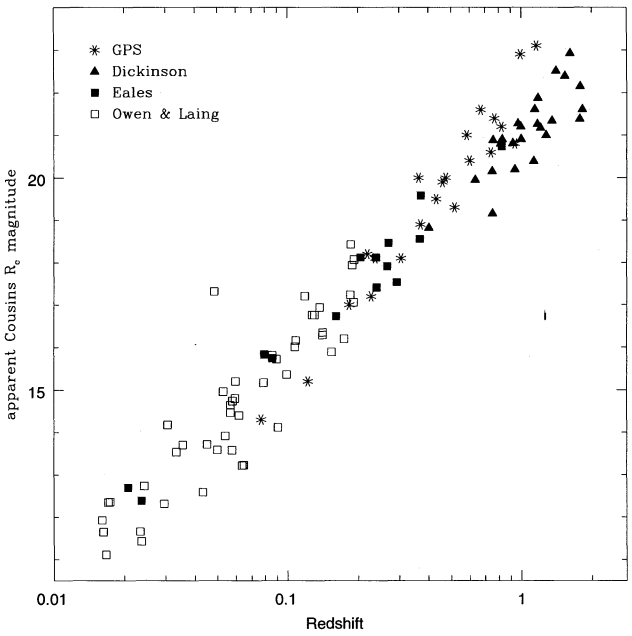

FIG. 2.—The Cousins R_C-band Hubble diagram for powerful radio galaxies. Magnitudes are not K-corrected. GPS galaxies are asterisks, extended radio galaxies from Owen & Laing (1989) are open squares, 3CR galaxies from Eales (1985) are filled squares, and 3CR galaxies from M. Dickinson (1995, private communication) are filled triangles.

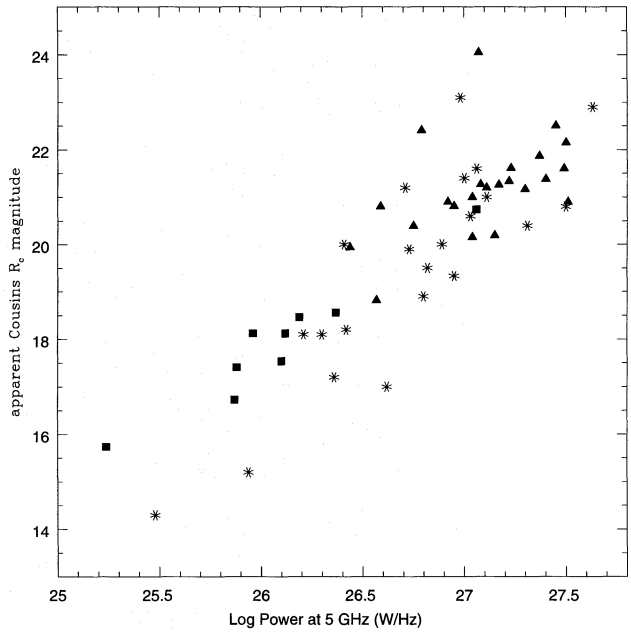

FIG. 3.—Apparent magnitude vs. log of radio power at 5 GHz (W Hz^{-1}). Symbols are as in Fig. 2.

extended sources are essentially the same. However, there is a suggestion that at redshifts of order unity, the 3CR galaxies are brighter by about 1 mag than the GPS galaxies. In addition, fits to the Hubble diagram (Table 3) show that the GPS galaxies have a steeper slope than the sample as a whole. The differences in the slopes of the fits to the GPS galaxies and the 3CR galaxies with $z \gtrsim 0.5$ is about 4 σ. Since the 3CR galaxies are now completely identified, the offset in magnitude is not due to incompleteness in the 3CR.

One possibility is that the extra light in the 3CR galaxies could be related to radio power—i.e., if the 3CR galaxies are stronger radio sources, then they may have more of the extra component. To investigate this, we have plotted the R_C magnitude versus radio power in Figure 3 for the GPS galaxies and the 3CR galaxies from Eales (1985) and M. Dickinson (1995, private communication). The optical magnitude increases as expected with increasing radio power because of the radio selection effects. However, there are no systematic differences between the GPS galaxies and 3CR galaxies. Thus, the result that, at high redshift, the 3CR galaxies are brighter than the GPS galaxies is not due to the 3CR galaxies having more powerful radio sources.

We have compared the data with models computed with the latest version of the Bruzual-Charlot population synthesis code (described by Charlot, Worthey, & Bressan 1996) assuming a single 0.5 Gyr duration burst of star formation at some formation redshift z_f, followed by "passive" evolution. The models are normalized in magnitude to the data at low redshift. The "no-evolution" model is that for an average elliptical at age 13.5 Gyr (see Fig. 5 of Bruzual & Charlot 1993). Figure 4 shows that the GPS galaxies are consistent with both the nonevolving elliptical model and passive evolution of an old stellar population ($z_f \gtrsim 5$). Models in which the stellar populations are younger (the

TABLE 3

FITS TO R_C HUBBLE DIAGRAM

Sample	Slope	Intercept
GPS galaxies	7.1 ± 0.2	22.2 ± 0.1
All galaxies	5.5 ± 0.1	20.8 ± 0.1
All galaxies $z \lesssim 0.5$	5.5 ± 0.2	21.3 ± 0.2
Non-GPS galaxies	5.2 ± 0.1	21.0 ± 0.1
Non-GPS galaxies $z \gtrsim 0.5$	5.1 ± 0.3	21.0 ± 0.1

NOTE.—Fits to the Hubble diagram of the form $m(R_C) =$ Intercept + Slope × log z.

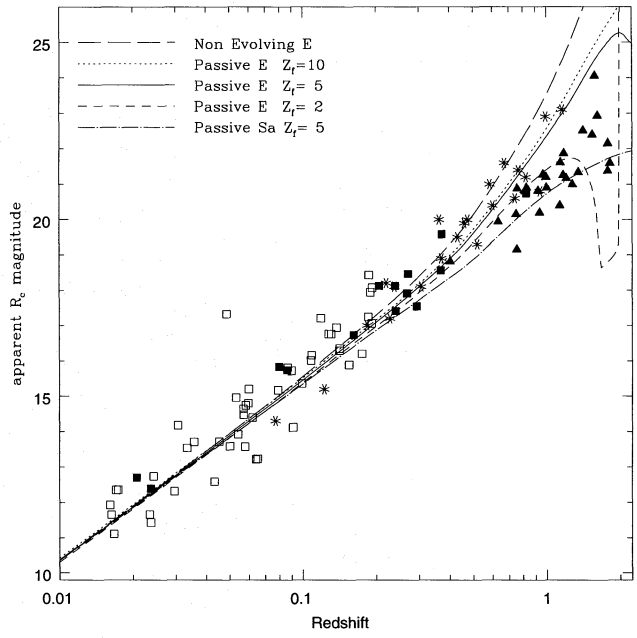

FIG. 4.—R_C-band Hubble diagram for powerful radio galaxies. Same data (and symbols) as in Fig. 2 but includes models from Bruzual & Charlot (1993). The key for the models is as follows (see § 3.3 for a discussion). *Long-dashed curve:* nonevolving E galaxy; *dotted curve:* E galaxy with $z_f = 10$; *solid curve:* E galaxy with $z_f = 5$; *short-dashed curve:* E galaxy with $z_f = 2$; *dot–long-dashed curve:* Sa galaxy with $z_f = 5$. All models assume $H_0 = 75$ and $q_0 = 0.1$.

Elliptical model with $z_f = 2$ and the Sa model with $z_f = 5$) tend to be brighter than the GPS sources at redshifts $z \approx 1$. The 3CR galaxies at $z \gtrsim 1$ are brighter than predicted by these passive evolution models with an old stellar population (see Spinrad 1986; Spinrad & Djorgovski 1987; Djorgovski 1987). The fact that the GPS galaxies agree with the models for passive evolution of old stellar populations suggests that difference between the GPS and 3CR galaxies is not due to the GPS galaxies being redder than normal elliptical galaxies, but to the 3CR galaxies being bluer than normal elliptical galaxies.

Recall that the *R*-band filter samples the 3000–4000 Å light at these redshifts. Thus, the fact that the 3CR galaxies are brighter than both the GPS galaxies and the simple passive evolution models could be due to the 3CR sources having an additional component of blue light that is not present in GPS galaxies (see also Snellen et al. 1996). This extra blue light in the 3CR sources could be the "aligned component" (McCarthy et al. 1987; Chambers, Miley, & van Breugel 1987; McCarthy 1993 and references therein). The aligned component could be (1) young stars from a "jet-induced starburst" (see, e.g., De Young 1989; Rees 1989; Daly 1990; Begelman & Cioffi 1989), (2) scattered nuclear continuum (Tadhunter, Fosbury, & di Serego Alighieri 1988; Fabian 1989), (3) inverse-Compton from the radio-emitting electrons (Daly 1992), or some combination of these.

The existing images of GPS host galaxies do not show strong evidence for an alignment effect. The lack of such a large-scale blue aligned component in the GPS sources could be due to the small subkiloparsec size of the radio source. The small size would prevent it from performing the roles that the large-scale radio sources in the 3CR galaxies are thought to play, i.e., (1) triggering a large-scale starburst, (2) clearing a path for ionizing photons to escape from the nucleus to illuminate gas clouds in the galaxy, or (3) providing an extended source of relativistic electrons for inverse-Compton scattering. If the blue light is mainly scattered nuclear light, then the GPS sources may be somewhat brighter in the IR than 3CR sources of comparable radio power. The *IRAS* data are consistent with any differences being smaller than a factor of a few (Heckman et al. 1994). This should be testable with the *Infrared Space Observatory*.

One consequence of this is that the stellar evolution of GPS galaxies may be simpler than the 3CR galaxies with large-scale radio sources. Thus, the GPS galaxies may be better "standard candles" in this regard.

3.4. *Color Evolution*

The reddening-orrected colors are plotted in Figure 5 as a function of redshift for those objects with measured $r - i$ color and measured redshift. We ignore objects with $|b| < 10°$ because of their large and uncertain corrections. Several models (described above) are plotted for comparison with the color data. At low redshift $z \lesssim 0.5$, there is not much difference in the elliptical models, and they are all in good agreement with the data. Although the elliptical models start to diverge at higher redshifts, there is significant scatter in the four data points, and it is not possible to distinguish between the elliptical models. However, the Sa galaxy is too blue to reproduce the GPS colors. Thus, we find that the majority of GPS galaxies have integrated $r - i$ colors that are consistent with those of passively evolving or nonevolving elliptical galaxies.

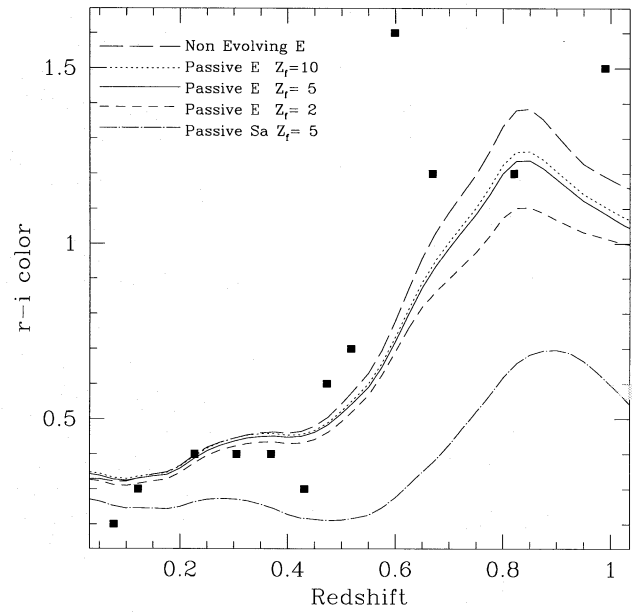

FIG. 5.—$r - i$ color vs. redshift for GPS host galaxies. The key to the plotted models is the following (see § 3.4 for a discussion). *Long-dashed curve:* nonevolving E galaxy; *dotted curve:* E galaxy with $z_f = 10$; *solid curve:* E galaxy with $z_f = 5$; *short-dashed curve:* E galaxy with $z_f = 2$; *dot–long-dashed curve:* Sa galaxy with $z_f = 5$. All models assume $H_0 = 75$ and $q_0 = 0.1$.

3.5. *Are There Unusually Red GPS Galaxies?*

We find that the $r - i$ colors of *most* GPS galaxies are consistent with those of elliptical galaxies whose stellar populations are old and either passively evolving or nonevolving. However, we find that three of the galaxies (0108+388, 0404+768, and 2128+048) are significantly redder than any of the models. This should be regarded as a tentative result because these are three of the faintest galaxies in our sample. Assuming that these galaxies are indeed unusually red, we consider three explanations for the colors and suggest it may be due to the presence of an obscured nucleus.

Dust in the whole galaxy.—If the three very red galaxies are red because of extra extinction, then the extra $E(B-V)$ needed is $\Delta E(B-V) \simeq 1.4$. Applying this correction to the observed *r* magnitude would make these galaxies about 2–3 mag brighter than 3CR radio galaxies. In addition, optical spectra of 0108+388 and 0404+768 (Lawrence et al. 1996) are not consistent with this much reddening. Thus, an interpretation in terms of extinction of the stellar light of the elliptical galaxy seems to be unlikely.

Emission lines in the i band.—For 2128+048, there are no candidates for bright emission lines in the *i*-band filter. For 0404+768 and 0108+388, in principle O III λ5007 could contribute to the flux; however, the observed equivalent widths are too low to account for the observed effect (Lawrence et al. 1996).

A truncated initial mass function in starburst galaxies.—Charlot et al. (1993) point out that a starburst that is deficient in low-mass stars will evolve to become very red when the turnoff mass reaches the lower cutoff in the IMF. This can be tested by searching for a very large 4000 Å break and spectral features from late-type giants. At this point this possibility seems ad hoc since it is not clear why these particular galaxies should have experienced a starburst with a cutoff to the low end of the IMF.

I-band light dominated by red nucleus; i.e., dust in the nucleus.—O'Dea et al. (1992) present evidence for a reddened nucleus in 0108+388 and 2322−040. In addition, G. Rieke (1995, private communication) reports variability in the K band in 0108+388 that is due to a strong nuclear component seen at that band. Thus, in these two GPS galaxies, there is evidence for an obscured nuclear component. This may also be the explanation for the red colors in 0404+687 and 2128+048. This hypothesis can be tested using near-IR imaging of these galaxies, which is in progress.

4. SUMMARY

We discuss the properties of the host galaxies of GPS radio galaxies using a sample of 40 GPS sources with CCD images. This sample includes six objects identified on the basis of their radio morphology as compact symmetric objects (Wilkinson et al. 1994; Readhead et al. 1996a, 1996b). The optical properties of these objects are consistent with those of the other GPS sources.

1. GPS galaxies show distorted morphologies and the presence of possible companions and are likely to be in interacting systems.

2. The absolute magnitudes of the GPS galaxies are in the range $-22.0 \lesssim R_C \lesssim -24.0$, consistent with the hosts of galaxies with powerful extended radio sources.

3. The colors of GPS galaxies are consistent with those of elliptical galaxies with an old stellar population that is either not evolving or evolving passively without active star formation. However, three galaxies appear to have colors that are redder than predicted by the models—this may be due to the presence of a reddened nucleus in the galaxy which contributes significantly to the i-band magnitude.

4. The GPS galaxies obey essentially the same R_C Hubble law as do the 3CR galaxies with powerful extended sources. There is a suggestion that at $z \gtrsim 0.5$, the GPS galaxies are fainter than the 3CR galaxies. This may be due to the 3CR galaxies at these redshifts being either brighter or bluer than the GPS galaxies. If the GPS galaxies are redder than the 3CR galaxies, this may be due to the lack of the blue light on the scale of tens of kiloparsecs (i.e., the aligned component) that is observed in high-redshift 3CR radio galaxies. The reason this aligned component is not present in GPS galaxies is not yet known. We suggest it may be due to the lack of extended radio sources that can (*a*) trigger star formation, (*b*) clear a path for nuclear light to illuminate and scatter off of clouds in the galaxy, or (*c*) generate inverse-Compton emission. Similar conclusions have also been reached by Snellen et al. (1996).

The above properties are consistent with the GPS galaxies being the progenitors of the 3CR radio galaxies. Additional work on the X-ray properties and the gas content of the host galaxies is needed to distinguish between those sources that may evolve to become classical doubles and those that remain frustrated on subkiloparsec scales.

This research made use of the NASA/IPAC Extragalactic Database (NED), which is operated by the Jet Propulsion Laboratory, California Institute of Technology, under contract with the National Aeronautics and Space Administration. We thank the referee for helpful comments. We are grateful to Tony Readhead and Greg Taylor for sharing unpublished data on the CSOs, Ignas Snellen for communicating his results prior to publication, Tim Heckman for comments on the manuscript, and Wim De Vries for helpful discussions and to the B. Ö. C. for inspiration.

REFERENCES

Bartel, N., Shapiro, I. I., Huchra, J. P., & Kühr, H. 1984, ApJ, 279, 112
Baum, S. A., & Heckmnan, T. 1989, ApJ, 336, 702
Baum, S. A., O'Dea, C. P., Murphy, D. W., & de Bruyn, A. G. 1990, A&A, 232, 19
Begelman, M. C., & Cioffi, D. F. 1989, ApJ, 345, L21
Biretta, J. A., Schneider, D. P., & Gunn, J. E. 1985, AJ, 90, 2508
Bruzual, G. A. 1981, Ph.D. thesis, Univ. California, Berkeley
Bruzual, G. A., & Charlot, S. 1993, ApJ, 405, 538
Burstein, D., & Heiles, C. 1982, AJ, 87, 1165
Carvalho, J. C. 1985, MNRAS, 215, 463
———. 1994, A&A, 292, 392
Chambers, K. C., Miley, G. K., & van Breugel, W. 1987, Nature, 329, 604
Charlot, S., Ferrari, F., Mathews, G. J., & Silk, J. 1993, ApJ, 419, L57
Charlot, S., Worthey, G., & Bressan, A. 1996, ApJ, 457, 625
Coleman, G. D., Wu, C.-C., & Weedman, D. W. 1980, ApJS, 43, 393
Daly, R. A. 1990, ApJ, 355, 416
———. 1992, ApJ, 386, L9
de Vries, W. H. 1995, Master's thesis, Univ. Groningen
de Vries, W. H., Barthel, P. D., & Hes, R. 1995, A&AS, 114, 259
de Vries, W. H., Barthel, P. D., Hes, R., & O'Dea, C. P. 1996, A&A, submitted
De Young, D. S. 1989, ApJ, 342, L59
———. 1993, ApJ, 402, 95
Djorgovski, S. 1987, in Nearly Normal Galaxies, ed. S. Faber (New York: Springer), 290
Dunlop, J. S., Peacock, J. A., Savage, A., Lilly, S. J., Heasley, J. N., & Simon, A. J. B. 1989, MNRAS, 238, 1171
Eales, S. A. 1985, MNRAS, 213, 899
Fabian, A. C. 1989, MNRAS, 238, 41P
Fanaroff, B., & Riley, J. 1974, MNRAS, 167, 31P
Fanti, C., Fanti, R., Dallacasa, D., Schilizzi, R. T., Spencer, R. E., & Stanghellini, C. 1995, A&A, 302, 317
Fanti, R., Fanti, C., Schilizzi, R. T., Spencer, R. E., Rendong, N., Parma, P., van Breugel, W. J. M., & Venturi, T. 1990, A&A, 231, 333
Fosbury, R. A. E., Bird, M. C., Nicholson, W., & Wall, J. V. 1987, MNRAS, 225, 761
Frei, Z., & Gunn, J. E. 1994, AJ, 108, 1476
Fugmann, W., & Meisenheimer, K. 1988, A&AS, 76, 145
Fugmann, W., Meisenheimer, K., & Röser, H.-J. 1988, A&AS, 75, 173
Gilmore, G. F., & Shaw, M. A. 1986, Nature, 321, 750
Heckman, T. M., O'Dea, C. P., Baum, S. A., & Laurikainen, E. 1994, ApJ, 428, 65
Heckman, T. M., Smith, E. P., Baum, S. A., van Breugel, W. J. M., Miley, G. K., Illingworth, G. D., Bothun, G. D., & Balick, B. 1986, ApJ, 311, 526
Hewitt, A., & Burbidge, G. 1991, ApJS, 75, 297
Hodges, M. W., & Mutel, R. L. 1987, in Superluminal Radio Sources, ed. J. A. Zensus & T. J. Pearson (Cambridge: Cambridge Univ. Press), 168
Hutchings, J. B. 1987, ApJ, 320, 122
Hutchings, J. B., Johnson, I., & Pyke, R. 1988, ApJS, 66, 361
Jauncey, D. L., White, G. L., Batty, M. J., & Preston, R. A. 1986, AJ, 92, 1036
Jiménez, E. P. 1987, Ph.D. thesis, Univ. Sussex
Kühr, H., Nauber, U., Pauliny-Toth, I. I. K., & Witzel, A. 1981a, Max-Planck-Institute für Radioastronomie, preprint no. 55
Kühr, H., Witzel, A., Pauliny-Toth, I. I. K., & Nauber, U. 1981b, A&AS, 45, 367
Lawrence, C. R., Pearson, T. J., Readhead, A. C. S., & Unwin, S. C. 1986, AJ, 91, 494
Lawrence, C. R., Readhead, A. C. S., Pearson, T. J., & Unwin, S. C. 1987, in Superluminal Radio Sources, ed. J. A. Zensus & T. J. Pearson (Cambridge: Cambridge Univ. Press), 260
Lawrence, C. R., et al. 1996, in preparation
Ledlow, M. J., & Owen, F. N. 1995, AJ, 110, 1959
McCarthy, P. J. 1993, ARA&A, 31, 639
McCarthy, P. J., van Bruegel, W., Spinrad, H., & Djorgovski, S. 1987, ApJ, 321, L29
Meisenheimer, K., & Röser, H.-J. 1983, A&AS, 51, 41
O'Dea, C. P. 1990, MNRAS, 245, 20P
O'Dea, C. P., Baum, S. A., & Morris, G. B. 1990a, A&AS, 82, 261
O'Dea, C. P., Baum, S. A., & Stanghellini, C. 1991, ApJ, 380, 66
O'Dea, C. P., Davies, J. K., Stanghellini, C., Baum, S. A., & Laurikainen, E. 1992, in AIP Conf. Proc. 254, Testing the AGN Paradigm, ed. S. S. Holt, S. G. Neff, & C. M. Urry (New York: AIP), 435
O'Dea, C. P., et al. 1996, in preparation
Owen, F. N., & Laing, R. A. 1989, MNRAS, 238, 357
Owen, F. N., & White, R. A. 1991, MNRAS, 249, 164

Pauliny-Toth, I. I. K., Witzel, A., Preuss, E., Kühr, H., Kellermann, K. I., Fomalont, E. B., & Davis, M. M. 1978, AJ, 83, 451
Peacock, J. A., Perryman, M. A. C., Longair, M. S., Gunn, J. E., & Westphal, J. A. 1981, MNRAS, 194, 601
Peacock, J. A., & Wall, J. V. 1982, MNRAS, 198, 843
Peterson, B. A., Savage, A., Jauncey, D. L., & Wright, A. E. 1982, ApJ, 260, L27
Phillips, R. B., & Mutel, R. L. 1982, A&A, 106, 21
Porcas, R. W. 1990, in Compact Steep Spectrum and GHz Peaked Spectrum Radio Sources, ed. C. Fanti, R. Fanti, C. P. O'Dea, & R. T. Schilizzi (Bologna: Istituto di Radioastronomia), 167
Postman, M., & Lauer, T. R. 1995, ApJ, 440, 28
Readhead, A. C. S., Taylor, G. B., Xu, W., Pearson, T. J., & Wilkinson, P. N. 1996a, ApJ, 460, 612
Readhead, A. C. S., Taylor, G. B., Xu, W., Pearson, T. J., Wilkinson, P. N., & Polatidis, A. G. 1996b, ApJ, 460, 634
Readhead, A. C. S., Xu, W., Pearson, T. J., Wilkinson, P. N., & Polatidis, A. G. 1994, in Compact Extragalactic Radio Sources (Proc. of NRAO Workshop 23), ed. J. A. Zensus & K. I. Kellermann (Greenbank: NRAO), 17
Rees, M. J. 1989, MNRAS, 239, 1P
Savage, B. D., & Mathis, J. S. 1979, ARA&A, 17, 73
Shaw, M. A., Tzioumis A. K., & Pedlar A. 1992, MNRAS, 256, 6P
Smith, E. P., & Heckman, T. K. 1989a, ApJS, 69, 365
———. 1989b, ApJ, 341, 658
Snellen, I. A. G., Bremer, M. N., Schilizzi, R. T., Miley, G. K., & van Oijk, R. 1996, MNRAS, 279, 1294
Spinrad, H. 1986, PASP, 98, 269
Spinrad, H., & Djorgovski, S. 1987, in IAU Symp. 124, Observational Cosmology, ed. A. Hewitt, G. Burbidge, & Zh.-F. Li (Dordrecht, Reidel), 129
Stanghellini, C. 1992, Ph.D. thesis, Univ. of Bologna.
Stanghellini, C., O'Dea, C. P., Baum, S. A., & Laurikainen, E. 1993, ApJS, 88, 1
Stickel, M., Rieke, M. J., Rieke, G. H., & Kühr, H. 1996, A&A, 306, 49
Stickel, M. & Kühr, H. 1993, A&AS, 100, 395
———. 1994, A&AS, 105, 211
Tadhunter, C. N., Fosbury, R. A. E., & di Serego Alighieri, S. 1988, in BL Lac Objects: Proc. of the Como Conference, ed. L. Maraschi, T., Maccacaro, & M.-H. Ulrich (Heidelberg: Springer), 79
van Breugel, W., Miley, G., & Heckman, T. 1984, AJ, 89, 5
Wilkinson, P. N., Booth, R. S., Cornwell, T. J., & Clark, R. R. 1984, Nature, 308, 619
Wilkinson, P. N., Polatidis, A. G. Readhead, A. C. S., Xu., W., & Pearson, T. J. 1994, ApJ, 432, L87